Scripta Materialia 237 (2023) 115709

Contents lists available at ScienceDirect

Scripta Materialia

journal homepage: www.journals.elsevier.com/scripta-materialia

Bonding mechanism and magnetic ordering in Laves phase λ_1-MgCo_2 intermetallic compound from theoretical and experimental studies

V.A. Yartys [a,*], P. Vajeeston [b], R.V. Denys [a], L. Havela [c], S. Maskova-Cerna [c], A. Szytula [d]

[a] Institute for Energy Technology, Kjeller, Norway
[b] University of Oslo, Norway
[c] Charles University, Prague, Czech Republic
[d] Jagellonian University, Cracow, Poland

ARTICLE INFO

Keywords:
Electronic structure
Bonding mechanism
Magnetic structure
Neutron powder diffraction
Covalent Co-Co bonding

ABSTRACT

In the present work we have studied the bonding mechanism and magnetism in a hexagonal λ_1-MgCo_2 Laves phase intermetallic formed at r_A/r_B= 1.280. *Ab initio* theoretical calculations for $MgCo_2$ using the projector-augmented wave method implemented in the VASP code showed that Mg carries a formal charge +1.7 |e| while Co atoms are also positively charged with around +0.7 |e| being donated to establish the interatomic covalent Co-Co bonding in a three-dimensional network of Co tetrahedra. $MgCo_2$ is a metallic conductor with ferromagnetic properties and T_C=303 K. Neutron Powder Diffraction study showed a collinear ordering of the Co moments, their alignment along the *c*-axis of the hexagonal unit cell with an average moment of 1.51(2) μ_B/atom Co. *Ab initio* computational studies indicate that the Co moments reach the experimentally observed value approx.1.5 μ_B when the unit cell volume exceeds 160 Å^3 (average Co-Co distances 2.43 Å).

Laves type AB_2 intermetallics belong to the most populated group of intermetallic compounds containing more than 10 hundred of representatives. The overwhelming majority of the Laves type intermetallics crystallizing with the C15 / FCC $MgCu_2$ or the C14 / hexagonal $MgZn_2$ type of structures are formed for a large range of ratios between the atomic radii of the A and B components outside the ideal ratio r_A/r_B= 1.225. In the present work we have studied the bonding mechanism, magnetic properties and crystal and magnetic structure of λ_1-MgCo_2 formed at r_A/r_B= 1.280. The material of choice is formed by A element Mg having a rather simple electronic structure of the valence electrons $2p^6 3s^2$ and a typical transition 3*d*- metal Co with a $3d^8 4s^1$ valence electrons outer shell. Recently, a comprehensive review paper describing various properties of the hydrogenated Laves type intermetallics as hydrogen storage materials has been published by the authors [1].

Earlier studies of the magnetic properties of $MgCo_2$ were reported in [2–4]. Ref. [2] suggested that $MgCo_2$ is a ferromagnet with T_C of 321 K which turns into antiferromagnetism at T = 45 K [2]. This has not been confirmed for the stoichiometric compound in a subsequent work [3], and the appearance of antiferromagnetism was attributed to the presence of a Co-deficient phase. *Ab initio* calculations (LMTO method with GGA approximation) yielded Co moments of 1.32 and 1.23 μ_B at the 6 h and 2*a* sites, and an induced negative moment of −0.17 μ_B at Mg [4]. This gives magnetization slightly smaller (2.43 μ_B/f.u. than the experimental value 1.3 μ_B/Co [2] (assuming no moment on Mg and equal moments on both Co sites).

Recently $MgCo_2D_3$ hydride was synthesized at 300 °C and a deuterium pressure of 2.8 GPa from a single phase $MgCo_2$ intermetallic alloy [5] resulting in the formation of the Mg_2CoD_5 deuteride and elemental Co. In the $MgCo_2$-D system, the phase-structural transformations occurring during the Hydrogenation-Disproportionation-Desorption-Recombination (HDDR) process at temperatures 27–500 °C were studied using in situ neutron powder diffraction (NPD) and showed that the Desorption-Recombination Process takes place leading to a complete recovery of the initial $MgCo_2$ intermetallic [5].

Chemically related hexagonal $MgNi_2$ Laves type intermetallic compound forms a trihydride $MgNi_2H_3$ and undergoes a hydrogen assisted phase transition into the orthorhombic $MoSi_2$-type structure with H atoms filling the deformed octahedra Mg_4Ni_2 and the positions within the buckled nets –Ni–H–Ni–H– penetrating through the structure and containing covalent Ni-H bonds [6,7].

The present work aims to establish the bonding mechanism, to probe the magnetic properties and to study the electronic, crystal, and magnetic structures of the $MgCo_2$ intermetallic.

* Corresponding author.
E-mail address: volodymyr.yartys@ife.no (V.A. Yartys).

https://doi.org/10.1016/j.scriptamat.2023.115709
Received 2 June 2023; Received in revised form 27 July 2023; Accepted 8 August 2023
Available online 11 August 2023

Experimental details describing preparation of the sample and the details of the Neutron Powder Diffraction, magnetization characterization and theoretical studies are presented in the Supplementary Information file.

1. Computational studies of the electronic structure of $MgCo_2$

The projector-augmented wave (PAW) [21] method describing the interaction between the core and the valence electrons ($2p^6 3s^2$ of Mg and $3d^8 4s^1$ of Co were considered as valence electron configurations) was implemented in the VASP code [8,9]. The Perdew, Burke, and Ernzerhof (PBE) functional [10] was used for the exchange-correlation term. The Hubbard parameter U was included in the rotationally invariant form [11,12]. Effective U value for the d states were chosen to be 3.2 eV for Co and the effective on-site exchange interaction J was fixed to 1 eV. Such values are in a ballpark of U and J used for Co in a metallic state. Resulting somewhat higher calculated Co moments are in a better agreement with experiment than the LMTO results using only GGA [4]. The optimized structures are obtained by minimizing both the stress tensor and the Hellman-Feynman forces, using the conjugate-gradient algorithm with an energy convergence threshold of 10^{-3} eV. Brillouin zone (BZ) integration was performed with Γ-centred Monkhorst-Pack grids. The size of reciprocal-space grids varies with the shape and the volume of the simulation cell. We found that an energy convergence within 20 meV is obtained using a k-points resolution of 0.1 $Å^{-1}$ and a 600 eV kinetic energy cutoff for the plane wave expansion. For each of the considered modifications, complete structural optimization (cell shape and volume, atomic positions) was performed.

Total, site and orbital Densities of State (DOS) calculated for the experimentally observed dimensions of the unit cell of $MgCo_2$ are presented in Fig. 1, a and b. From the presented data it is clear that DOS is dominated by the Co-3d contributions, with very similar behaviours for Co1 and Co2. In contrast, the Mg states and Co-s and Co-p states all show a marginal contribution to the DOSs.

Path in the Brillouin Zone of the electronic structure of $MgCo_2$ is shown in Figure S1 (Suppl. Information file).

In the $MgCo_2$ lattice an electron density is transferred from Mg and Co, as can be clearly seen in the Fig. 2a. Furthermore, a significant preference in charge density localization between the Co1-Co2/Co1-Co1 atoms, as compared with Mg-Co and Mg-Mg atoms (Fig. 2b), can be observed. The charge transfer involving the spatial framework of Co atoms built from Co_4 tetrahedra exhibits an anisotropic pattern, see Fig. 2b. From Fig. 2c, one can deduce a negligibly small ELFs between the Co and Mg atoms, and small values of ELF at the Co sites. In contrast, it can be inferred that high values of ELF between the Co atoms indicate presence of strongly paired electrons with local bosonic character. This feature can be related to the effect of Co 3d-electrons while a non-spherical distribution of ELF indicates that the bonding between the Co atoms is dominated by covalent interactions. Indeed, the anisotropic charge transfer and nonspherical distribution of electron density amongst the Co sites is in line with the strong covalent Co-Co bonding.

The calculated Mulliken effective charges (MEC) values for Mg, Co (1) and Co(2) are +1.72|e|, +0.72 and +0.71|e|, respectively. That means that electronic charges are transferred both from the Mg and Co atoms. The charge transfer can be related to the donation of appr. 2 electrons by each Mg atom and 1 s-electron by each Co atom. The redistributed charges form Co-Co covalent bonds.

2. Magnetic properties of $MgCo_2$

The temperature and field dependences of the magnetization were measured in the temperature range 2 – 313 K (Quantum Design PPMS 14 equipment). The material appeared to be ferromagnetic. The spontaneous moment of 2.6 μ_B/f.u. was deduced from the field dependence of magnetization (Fig. 3a) which corresponds to 1.3 μ_B/Co [2]. The saturation of magnetization occurs in fields lower than 1 T, while it shows some temperature variations in lower fields. The hysteresis is negligible.

The temperature dependences of magnetization measured in the fields $\mu_0 H = 3$ and 6 T (Fig. 3b) indicate that the Curie temperature is close to room temperature. To determine it more precisely, we performed an ac-susceptibility measurement, $\chi_{ac}(T)$ using the ac field of 0.001 T and frequency 333 Hz. The results are shown in Fig. 3c. The Curie temperature can be derived from the inflection point of the real part $\chi'(T)$ appearing at 303±2 K. This is somewhat lower than T_C of 321 K reported in [2]. The fact, that $\chi_{ac}(T)$ forms a long plateau below T_C, and $\chi''(T)$ is not concentrated around T_C, indicates a weak anisotropy, evident already from the lack of hysteresis.

We did not observe any phase transformation at low temperatures,

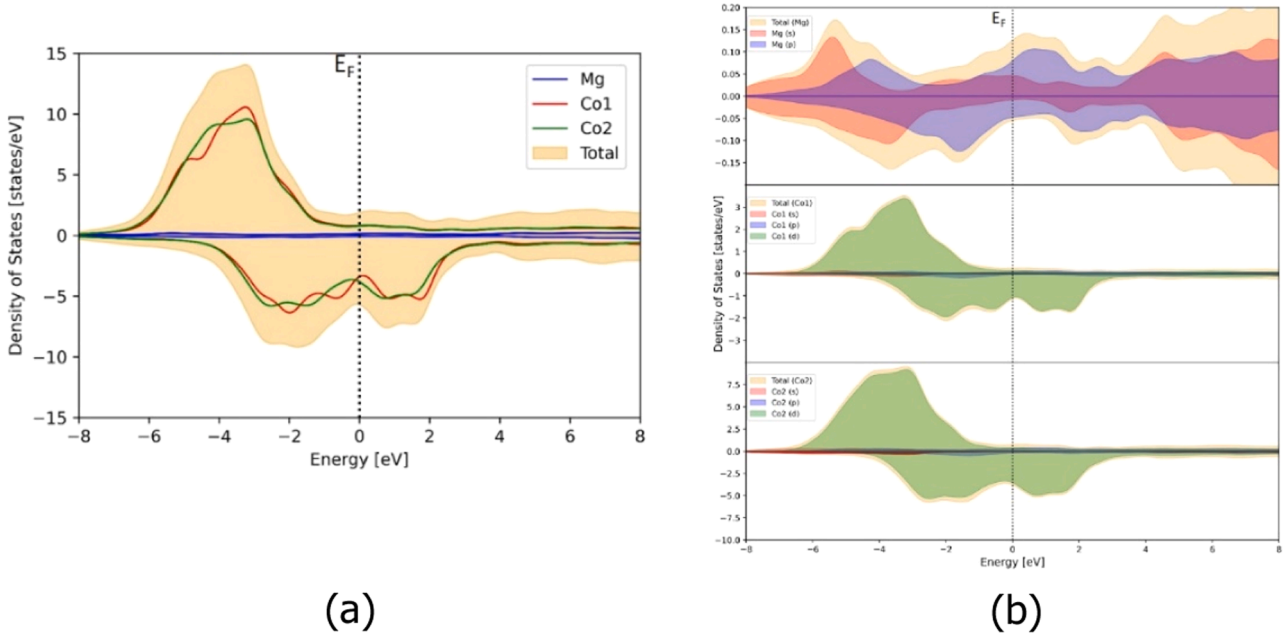

Fig. 1. (**a**) Calculated total and site projected density of states for $MgCo_2$. The Fermi level (E_F) is set to zero energy. (**b**) Calculated orbital projected density of states for $MgCo_2$. The Fermi level (E_F) is set to zero energy.

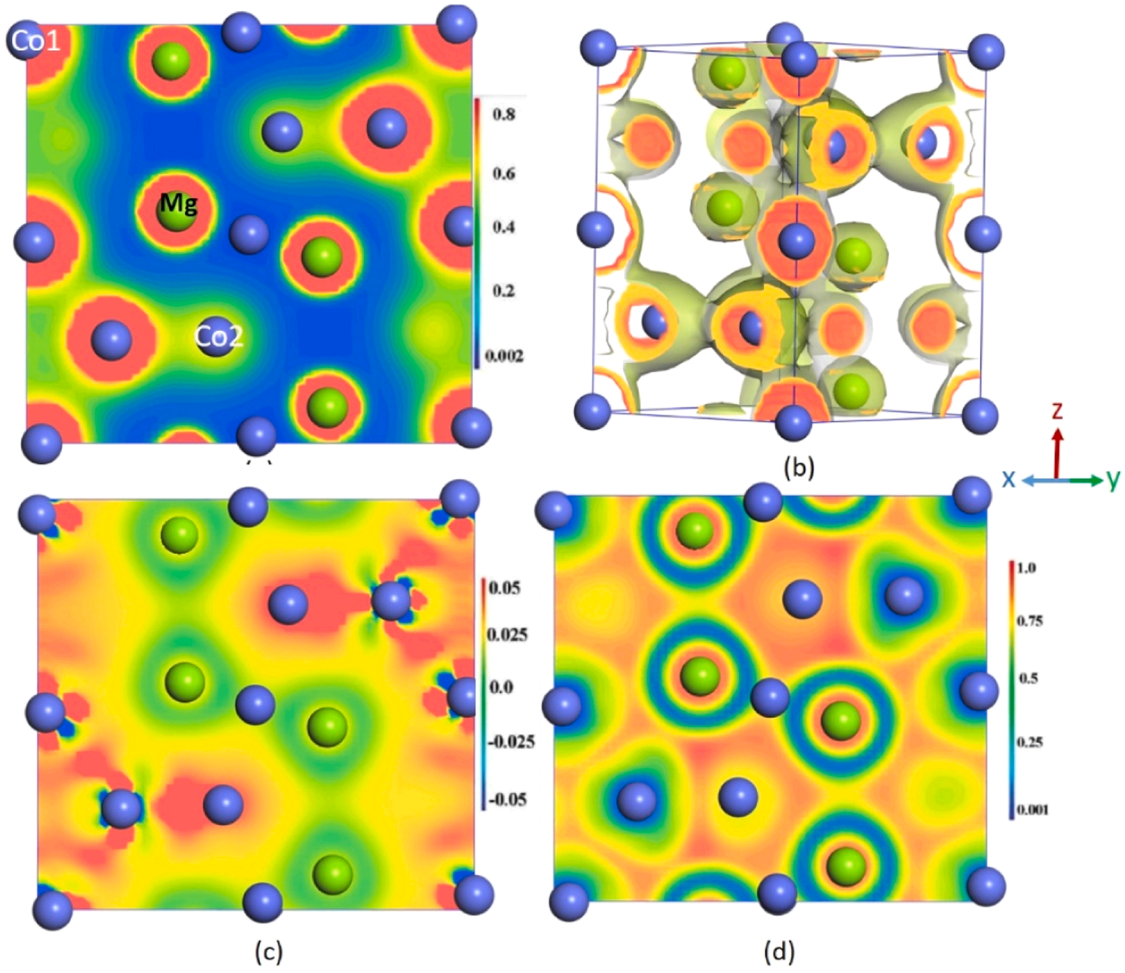

Fig. 2. Calculated charge density map for $MgCo_2$ in the (111) plane (a); a three-dimensional map of charge density distribution for $MgCo_2$ (b); charge transfer map for $MgCo_2$ in the (111) plane (c); and electron localization function for $MgCo_2$ in the (111) plane (d) plots.

hence the ground state is ferromagnetic.

3. Crystal and magnetic structures of λ_1-MgCo_2 from neutron powder diffraction studies

X-Ray diffraction studies (85 K) (Figures S1 and S2; Tables S1 and S2) and neutron powder diffraction pattern collected above the temperature of magnetic ordering both showed a presence of a single phase stoichiometric hexagonal Laves type λ_1-MgCo_2 intermetallic compound (85 K; $a = 4.8532(2)$; $c = 7.9260(3)$ Å), with a trace of MgO present as an admixture formed during the sintering process.

Fig. 4a shows the NPD pattern collected using the wavelenght λ=1.494 Å while Figure S3 together with the Table S3 characterizes the calculated NPD pattern. The refinements showed an excellent agreement between the experimental data and calculated intensities. The results of the refinements are listed in Table 1.

At $T = 2$ K, i.e. in the ordered state, no extra peaks appeared in the NPD pattern. However, intensities of particular peaks at lower angles significantly increased indicating magnetic contribution to the NPD diffraction pattern (see Fig. 4a).

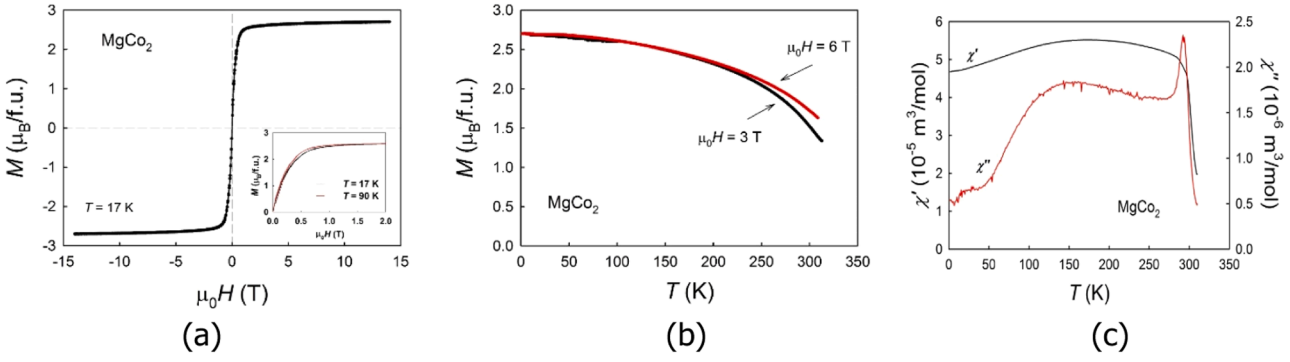

Fig. 3. (**a**) Hysteresis loop of $MgCo_2$ measured at $T = 17$ K. The inset shows a low field data at $T = 17$ and 90 K. (**b**) Temperature dependence of magnetization measured for $MgCo_2$ in magnetic fields of 3 and 6 T. (**c**) Temperature dependence of ac-susceptibility (real part, χ', and imaginaty part, χ'') of $MgCo_2$.

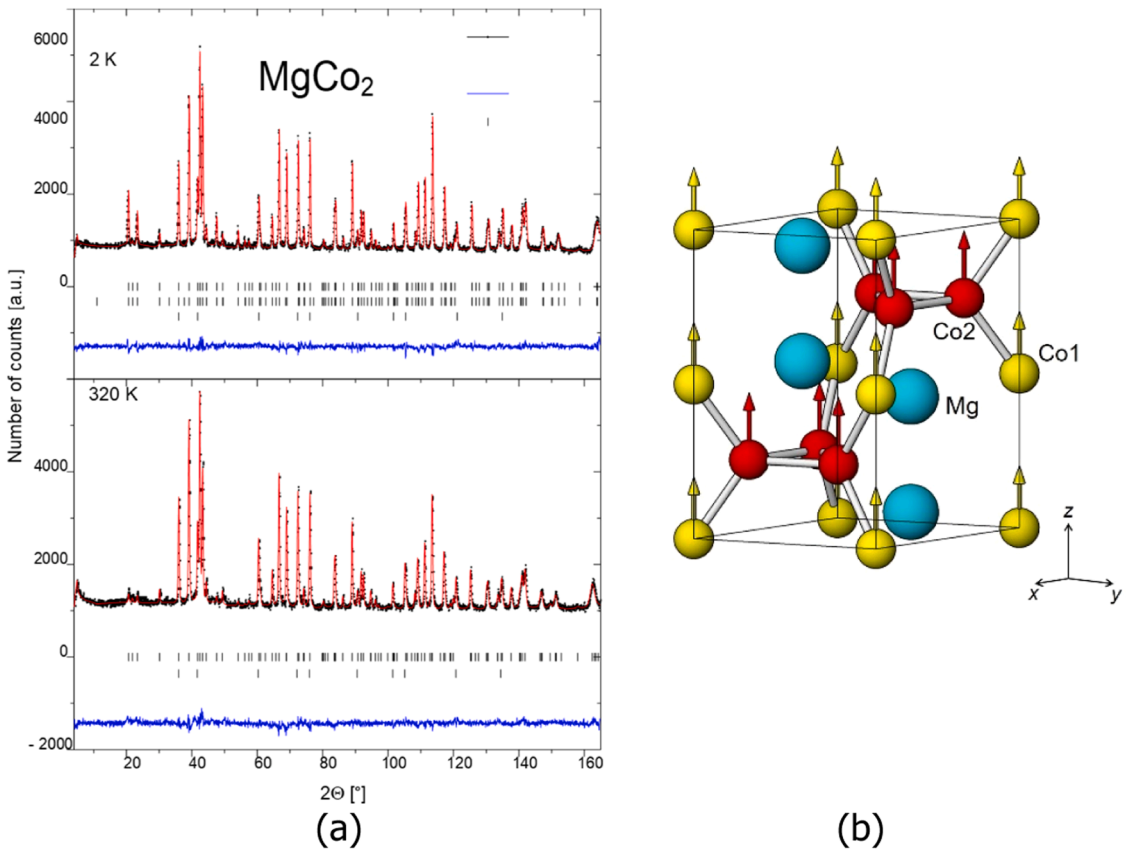

Fig. 4. (**a**) NPD pattern collected for $MgCo_2$ at $T = 320$ K (bottom) and 2 K (top). λ=1.494 Å, 2θ range 3.85–164.75°, step 0.05° Vertical ticks show the position of the Bragg peaks of the constituents: nuclear contribution for $MgCo_2$ (top in (a) and (b)); stainless steel sample holder (bottom in (a) and (b)); magnetic peaks for $MgCo_2$ (middle in (a)). (**b**) Magnetic ordering in $MgCo_2$ Laves λ_1-type intermetallic compound. In the ferromagnetically ordered structure Co atoms carry magnetic moments alligned along [001] with an average size of 1.51 μ_B and a slight difference in magnitude between two crystallographic sites, 1.31 μ_B (2*a* site) and 1.58 μ_B (6*h* site).

Rietveld refinements of the XRD and NPD data measured at 2 K, 85 K and 320 K showed that small contraction of the unit cells proceeds on cooling down from 320 K to 85 K and then to 2 K (see Table S4).

Refinement of the magnetic structure of $MgCo_2$ proved that it is ferromagnetic with magnetic moments carried by the Co atoms alligned along the *c*-axis of the hexagonal unit cell. Two possibilities have been tested.

(a) Magnetic moments of Co on both sites having the same values. The refinements gave 1.47(1) μ_B and yielded the magnetic R factor of 9.18%.
(b) Magnetic moments of Co at different sites, 6*h* and 2*a*, were allowed to vary independently. This gave 1.31(2) μ_B (2*a*) and 1.58(2) μ_B (6*h*) and resulted in lowering the R_{mag} to 6.67%. Thus, we concluded that the last model yielding an average values of magnetic moment of 1.51(2) μ_B /atom Co was the most suitable to describe the magnetic structure of $MgCo_2$.

The magnetic structure of $MgCo_2$ is shown in Fig. 4b.

4. Discussion and concluding remarks

Co-containing intermetallics exhibit a large diversity of magnetic properties. Co ions can be either magnetic or non-magnetic, depending on particular chemical composition and type of magnetic structure. The example of cubic Laves phases with rare earths is a nice illustration of importance of the shortest Co-Co spacing $d_{Co\text{-}Co}$ [13] in defining the magnetism in the $REMCo_2$ intermetallics. In particular, if $d_{Co\text{-}Co}$ is below 2.54 Å, Co atoms are non-magnetic unless the Co moments are supported by magnetic fields of by 4*f*-3*d* exchange interactions.

The 3*d*-4*d* hybridization can be tentatively taken as a reason why a well-studied hexagonal Laves phase $NbCo_2$ with a rather small unit cell (a = 4.80 Å, c = 7.90 Å [14]) has no stable magnetic moment on Co.

The situation in the relatively less abundant hexagonal Laves phases with Co is more complex due to two different Co sites and presence of Co-Co spacings with different multiplicities (see Table 1). The shortest

Table 1
Results of the Rietveld powder profile refinements of the nuclear and magnetic structure of $MgCo_2$ at $T = 320$ K and 2 K. HRPT, SINQ, PSI, λ=1.494 Å, 2θ range 3.85–164.75°, step 0.05°

Temperature	Unit cell parameters and space group	Atomic coordinates	*B*, Å^2
320 K	a = 4.85493(12) Å	4 Mg in 4*f*: 1/3, 2/3, *z*;	0.787 (21)
	c = 7.94124(19) Å	z = 0.06353(13);	0.493 (49)
	V = 162.10 Å^3	2 Co1 in 2*a*: 0,0,0;	0.579 (27)
	$P6_3/mmc$	6 Co2 in 6*h*: *x*,-*x*,1/4;	
	$d_{Co1—Co1}$ = 3.971 Å	x = 0.83003(26)	
	$d_{Co1—Co2}$ = 2.446 Å		
	$d^1_{Co2—Co2}$ = 2.379 Å		
	$d^2_{Co2—Co2}$ = 2.476 Å		
2 K	a = 4.85168(6) Å	z_{Mg} = 0.06316(11);	0.4
	c = 7.92123(15) Å	x_{Co2} = 0.83021(24)	0.4
	V = 161.48 Å^3		
	$P6_3/mmc$; R = 6.67%		
	$d_{Co1—Co1}$ = 3.961 Å		
	$d_{Co1—Co2}$ = 2.441 Å		
	$d^1_{Co2—Co2}$ = 2.380 Å		
	$d^2_{Co2—Co2}$ = 2.471 Å		

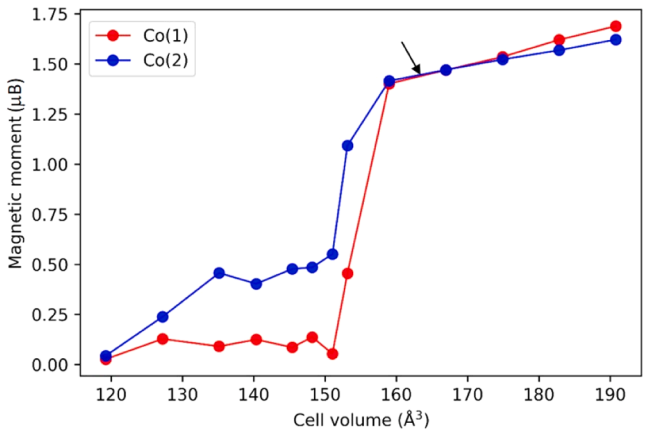

Fig. 5. Calculated magnetic moments of Co1 (2*a*) and Co2 (6*h*) as a function of unit cell volume. Experimental unit cell volume of 162.1 Å^3/unit cell is marked by an arrow.

Co-Co distance in $MgCo_2$, $d^1_{Co2—Co2} = 2.379$ Å, but the next shortest Co-Co distance of 2.446 Å, is also below the threshold of 2.54 Å mentioned above. Hence, the ferromagnetism of $MgCo_2$ appears to be rather unexpected. However, one has to consider that $MgCo_2$ does not have 5*d* states present in the rare-earth containing systems, which can hybridize with the Co-3*d* states and contribute to the electron delocalization.

Ab initio computational studies performed in this work revealed that the ferromagnetic ordering in $MgCo_2$ is indeed controlled by the interatomic spacings in the cobalt sublattice. A rapid growth of the value of μ_B/Co occurs after the theoretically assumed volume of the unit cell exceeds 153 Å^3 (38.2 Å^3/f.u.) (see Fig. 5). The onset of magnetism induced by the volume expansion can be taken as result of the narrowing of the *d*-band and increase of the density of states at the Fermi level in non-spin-polarized state.

For the volume exceeding 160 Å^3 (this corresponds to the average Co-Co distance of 2.43 Å) both Co sites have almost identical moments, close to the experimentally observed 1.5 μ_B. Due to the filling of the majority (spin-up) band, any further increase is rather small. The Co moments only would give a higher spontaneous magnetization than the value from the bulk magnetization study. However, the bulk value may be affected by opposite spin polarization of Mg states [2], invisible by neutron diffraction due its diffuse character.

The calculations prove that the electronic structure of $MgCo_2$ is significantly different from the $RECo_2$ intermetallics. Namely, the ferromagnetic ordering in $MgCo_2$ appears at much shorter Co-Co distances as compared to $RECo_2$. A comparison of the data of the computational studies performed in this work and those in the reference publication [4] concludes that the present study allowed to uncover the mechanism of the chemical bonding in the intermetallic alloy $MgCo_2$ which is associated with the formation of covalent Co-Co bonds within the framework of Co_4 tetrahedra making a framework of the structure of the studied Laves type C14 alloy. A detailed comparison of the results of two works is given in Table S5.

The covalent Co-Co bonding appears to be an interesting feature of the studied intermetallic alloy, which can be the reason for a very difficult hydrogenation of $MgCo_2$, requiring kBar level of hydrogen pressure and high temperatures, similar to the behaviour of the $MgNi_2$ intermetallic [5–7].

Declaration of Competing Interest

The authors declare that they have no known competing financial interests or personal relationships that could have appeared to influence the work reported in this paper.

Acknowledgements

This work is based on experiments performed at HRPT, Swiss Spallation Neutron Source SINQ, Paul Scherrer Institute, Villigen, Switzerland.

We are grateful to Dr. Denis Sheptyakov (Paul Scherrer Institute) for his help during the experiments at PSI.

We are grateful to Prof. V.E. Antonov (ISSPh RAS) for the measurements of the XRD data of $MgCo_2$.

We thank Prof. Chubin Wan (IFE and University of Science and Technology Beijing, China) for collaboration in neutron scattering studies of Mg-containing intermetallics and their hydrides.

We thank Dr. Bogusław Penc (Jagellonian University) for the collaboration in elaboration of the neutron diffraction data.

Supplementary materials

Supplementary material associated with this article can be found, in the online version, at doi:10.1016/j.scriptamat.2023.115709.

References

[1] Volodymyr A. Yartys, Mykhaylo V. Lototskyy, Laves type intermetallic compounds as hydrogen storage materials: a review, J. Alloy Comp. 916 (2022), 165219, https://doi.org/10.1016/j.jallcom.2022.165219.

[2] K.H.J. Buschow, Magnetic properties of $MgCo_2$, $MgNi_2$ and Mg_2Ni, Solid State Commun. 17 (1975) 891–893, https://doi.org/10.1016/0038-1098(75)90745-0.

[3] K.H.J. Buschow, H. Kropp, E. Dorman, Magnetic properties of $MgCo_2$ studied by means of magnetic dilution and ^{59}Co spin echo NMR, J. Magn. Magn. Mater. 23 (1981) 257–264, https://doi.org/10.1016/0304-8853(81)90045-7.

[4] H. Yamada, H. Shimizu, Magnetic states of $MgCo_2$ and $CaCo_2$ with the cubic and hexagonal Laves phase structures, J. Alloys Comp. 388 (2005) 15–18, https://doi.org/10.1016/j.jallcom.2004.07.002.

[5] ChuBin Wan, V.E. Antonov, R.V. Denys, V.I. Kulakov, V.A. Yartys, $MgCo_2$-D_2 and MgCoNi-D_2 systems synthesized at high pressures and studied by *in-situ* neutron powder diffraction during the HDDR processing, Prog. Nat. Sci. Mater. Int. 27 (1) (2017) 74–80, https://doi.org/10.1016/j.pnsc.2017.01.007.

[6] V.A. Yartys, V.E. Antonov, A.I. Beskrovnyy, J.C. Crivello, R.V. Denys, V.K. Fedotov, M. Gupta, V.I. Kulakov, M.A. Kuzovnikov, M. Latroche, Yu.G. Morozov, S. G. Sheverev, B.P. Tarasov, Hydrogen-assisted phase transition in a trihydride $MgNi_2H_3$ synthesized at high H_2 pressures: thermodynamics, crystallographic and electronic structures, Acta Mater 82 (2015) 316–327, https://doi.org/10.1016/j.actamat.2014.09.012.

[7] V.A. Yartys, V.E. Antonov, D. Chernyshov, J.C. Crivello, R.V. Denys, V.K. Fedotov, M. Gupta, V.I. Kulakov, M. Latroche, D. Sheptyakov, Structure and chemical bonding in $MgNi_2H_3$ from combined high resolution synchrotron and neutron diffraction studies and ab initio electronic structure calculations, Acta Mater 98 (2015) 416–422, j.actamat.2015.07.053.

[8] G. Kresse, J. Furthmüller, Efficient iterative schemes for ab initio total-energy calculations using a plane-wave basis set, *Phys. Rev.* B 54 (1996) 11169, https://doi.org/10.1103/PhysRevB.54.11169.

[9] G. Kresse, J. Furthmüller, Efficiency of ab-initio total energy calculations for metals and semiconductors using a plane-wave basis set, Comput. Mater. Sci. 6 (1996) 15–50, https://doi.org/10.1016/0927-0256(96)00008-0.

[10] J.P. Perdew, K. Burke, M. Ernzerhof, Generalized gradient approximation made simple, Phys. Rev. Lett. 77 (1996) 3865, https://doi.org/10.1103/PhysRevLett.77.3865.

[11] A.I. Liechtenstein, V.I. Anisimov, J. Zaanen, Density-functional theory and strong interactions: orbital ordering in Mott-Hubbard insulators, *Phys. Rev.* B 52 (1995) R5467, https://doi.org/10.1103/PhysRevB.52.R5467.

[12] S.L. Dudarev, G.A. Botton, S.Y. Savrasov, Z. Szotek, W.M. Temmerman, A. P. Sutton, Electronic structure and elastic properties of strongly correlated metal oxides from first principles: LSDA + U, SIC-LSDA and EELS study of UO_2 and NiO, Phys. Stat. Solidi A 166 (1998) 429–443, https://doi.org/10.1002/(SICI)1521-396X(199803)166:1<429::AID-PSSA429>3.0.CO;2-F.

[13] N.H. Duc, P.E. Brommer, K.H.J. Buschow, Handbook of Magnetic Materials, 12, Elsevier Science B.V., 1999, pp. 259–394.

[14] The Materials Project. Materials data on $NbCo_2$ by materials project, United States, 2020, https://doi.org/10.17188/1757277.